DETECTION OF PINE PROCESSIONARY MOTH (THAUMETOPOEA WILKINSONI) NESTS USING DEEP LEARNING

Fatih GENÇTÜRK[1]*, Cemal IŞILAK[2], İsmail Serkan ÜNCÜ[3]

[1]Isparta University of Applied Sciences, Faculty of Technology, Department of Computer Engineering, 32260, Isparta, Türkiye
[2]Erzincan Binali Yildirim University, Ali Cavit Çelebioğlu Civil Aviation College, Department of Avionics, 24002, Erzincan, Türkiye
[3]Isparta University of Applied Sciences, Faculty of Technology, Department of Electrical-Electronic Engineering, 32260, Isparta, Türkiye

Abstract: The pine processionary moth, widely found in Southern and Central Europe, North Africa, and the Middle East, causes significant economic and ecological losses in forests. This pest feeds on the needles of pine species, posing a greater threat than forest fires in Türkiye, where a large portion of the timber resource is made up of pine trees. This study aims to detect nests of the pine processionary moth residing on trees. A custom dataset was created using aerial images of infested pine trees. A deep learning model was trained using this dataset to facilitate nest detection. Using the YOLOv7 network, training and testing were performed on two datasets of different sizes. The analysis revealed that the dataset with a larger number of images yielded better performance in detecting pine processionary moth nests. The detection success of the model for nests was measured as 92.5% based on the mAP@0.5 metric. The findings of this study demonstrate the effectiveness of the proposed method for accurate and high-resolution detection of pine processionary moth nests in forestry applications. Moreover, these findings highlight the method's potential to support pest density monitoring and the identification of intervention priority areas. Future research should investigate the applicability of the proposed approach to other pest species and explore its integration into real-time monitoring and pest management systems for large-scale operations.

Keywords: Pine processionary moth, Deep learning, YOLOv7, Artificial intelligence, Forest pests, Classification

*Corresponding author: Isparta University of Applied Sciences, Faculty of Technology, Department of Computer Engineering, 32260, Isparta, Türkiye
E mail: fatihgencturk@isparta.edu.tr (Fatih GENÇTÜRK)

Fatih GENÇTÜRK	https://orcid.org/0000-0001-8557-5572	
Cemal IŞILAK	https://orcid.org/0000-0002-2445-0220	
İsmail Serkan ÜNCÜ	https://orcid.org/0000-0003-4345-761X	

1. Introduction

Forest pests can significantly hinder forest development. While fires are often considered the greatest threat to forests, insects can cause damage that exceeds the harm inflicted by fires both globally and in Türkiye (Özdal, 2002).

The Pine Processionary Moth (PPM), prevalent in the Middle East, Central and Southern Europe, and North Africa, has emerged as one of the most destructive pests in Türkiye. Its presence persists in Mediterranean, Aegean, Black Sea, and Marmara regions. The PPM damages several pine species, including red pine (Pinus brutia), black pine (Pinus nigra), Scots pine (Pinus sylvestris), Aleppo pine (Pinus halepensis), maritime pine (Pinus pinaster), and stone pine (Pinus pinea) (Özay, 2004).

PPM primarily damages trees during its larval stage, where the larvae feed on the needles of pine species. When their numbers reach sufficient levels, they can defoliate the trees completely. Trees infested with PPM larvae exhibit significantly reduced photosynthesis compared to non-infested counterparts due to their lack of leaves (Babur, 2002).

Larvae of PPM can typically be observed in higher elevations after the first half of August. These caterpillars feed on the nearest needles, forming silken nests. As the larvae develop, they may shift to new shoots, feeding on additional needles and forming sturdier, larger second nests. This cycle continues until the formation of a fourth nest. By this stage, the larvae have consumed all the needles, leaving only the stubs. With 150 to 300 larvae found in these nests, caterpillars rest during the day and emerge at night to feed. The increase in needle consumption occurs as the larvae molt five times throughout the fall and winter, leading to greater damage to the trees. The transition of larvae to the pupal stage begins in higher elevations by the end of March and occurs in lower elevations by May (Çanakçıoğlu, 1993; Yüksel, 2019).

Significant damage from PPM has been reported, reducing tree development by 24% in diameter, 36% in height, and 54% in total growth (Carus, 2004). Similarly, annual growth in slash pine forests has decreased by 34.6% to 39.7%, with subsequent years showing a decline of 43.1% to 58.3% (Avcı and Altunışık, 2016). In another study analyzing the loss in diameter and volume

growth of red pine trees affected by PPM, three different test sites were identified. The analysis showed that the loss in height and diameter growth at breast height was 35%, 50%, and 55% for the three sites, respectively. Similarly, the loss in volume growth was found to be 17%, 37%, and 44% (Erkan, 2011). In a separate study conducted to understand the impact of PPM on biomass growth, 30 maritime pine samples were analyzed. The reduction in biomass growth caused by PPM was reported to range between 37% and 73% on average (Arnaldo et al., 2010). In Türkiye, approximately 56% of forest areas consist of pine trees. Given that PPM negatively impacts the development of these forests, effective combat against the pest is of vital importance (Özay, 2004). Control measures against PPM include mechanical, chemical, biological, and biotechnical methods. Mechanical control involves removing the pest from its environment regardless of its life stage, typically by collecting egg sacs and winter nests and disposing of them far from their host trees. Biotechnical control aims to capture PPM using pheromone traps during the adult's active period from July to September. Chemical control seeks to eliminate PPM when it spreads across large areas, employing stomach and contact insecticides. Various chemicals are used for this purpose. Biological control involves utilizing natural enemies such as fungi, viruses, bacteria, birds, insects, plant oils, parasitoids and predators, and microbial pathogens to curb the pest population (Cebeci et al., 2010; Anonymous, 2016).

Timely detection of harmful species is crucial in the fight against forest pests. Early identification of harmful species helps protect tree health and maintain ecological balance by facilitating the implementation of necessary preventive measures. Further, the surveillance of temporal and spatial effects of pests is required for maximizing the efficiency of control tactics and for priority setting. In this strategy, a number of studies are being carried out that employ a range of techniques and methodologies, with particular focus on aerial photography analysis.

Gooshbor et al. (2016) analyzed the invasion of the green oak leaf roller (Tortrix viridana) in Zagros oak forests. Landsat satellite images were used for this purpose. The NDVI (Normalized Difference Vegetation Index) values from pre- and post-invasion periods were compared. The results showed a significant decrease in NDVI values during the post-invasion period compared to the pre-invasion period. The analysis demonstrated that NDVI values can be effectively used to monitor green oak leaf roller infestations.

Cardil et al. (2017) conducted a study in a pine forest in Spain to assess tree damage caused by PPM. Images captured using a drone equipped with an RGB (Red, Green, Blue) sensor were analyzed. Image processing was performed with the help of the "Agisoft Photoscan Professional" software. Using MLC (Maximum Likelihood Classification), trees were classified based on the extent of leaf damage caused by the infestation. Three different classes were defined for tree-based classification: non-infested, partially infested, and fully infested trees. The classification achieved an accuracy rate of 79%. Ziya et al. (2018) conducted a study involving image analysis to detect the presence and severity of leaf spot disease in a sugar beet field. RGB images of the field were captured using a drone. The study utilized 12 representative classes to determine the severity of the disease. Images were taken from a height of 30–60 cm above the ground, depending on plant height and lighting conditions, and were analyzed using the Matlab image processing library. The image processing was performed in the Lab color space. Disease severity was determined through operations such as K-means clustering, pixel labeling, segmentation, and contrast enhancement. The results were compared with expert assessments and found to be highly consistent.

Cardil et al. (2019) examined and classified the impact of PPM infestation on defoliation in pine and oak trees. The study, conducted in Spain, collected aerial images of trees using a drone equipped with RGB and multispectral sensors. Tree defoliation was analyzed using NDVI and ExG (Excess Green) indices derived from the images. For tree-based classification, three different classes were defined: non-defoliated, partially defoliated, and fully defoliated trees. The classification achieved an accuracy rate of 81.8%. Kerkech et al. (2020) conducted a study on the detection and mapping of mildew disease in vineyards located in France. Images were captured using a drone equipped with RGB and infrared sensors. The proposed method is based on the fusion of RGB and infrared images. Deep learning was used to distinguish between healthy and diseased areas, as well as shadow and ground sections in the images. The study employed the SegNet architecture, which was found to be suitable for detecting and mapping the disease. The method achieved an accuracy rate of 87% at the leaf level and 92% at the vine level. Chen et al. (2021) developed an intelligent pest management system for controlling Tessaratom papillosa. This study, conducted in Taiwan, utilized an exploratory drone to capture RGB images and an agricultural drone for spraying operations. To enable real-time image processing, an NVIDIA Jetson TX2 board was used to run the Tiny-YOLOv3 deep learning algorithm. A spraying map was generated to allow farmers to monitor pest distribution in real time and take preventive actions. Pest locations detected from the images were used to determine the optimal spraying route. The proposed model significantly improved efficiency compared to conventional spraying methods by reducing pesticide consumption, time spent, and total labor requirements. The study reported a reduction of 87.5% in pesticide use, 53% in spraying time, and 50% in required labor.

Akıncı and Göktoğan (2022), in their recent study, carried out a study in Eskişehir aimed at identification and mapping of PPM nests. A quadcopter equipped with four motors and an RGB sensor was used in the study for

image acquisition. According to acquired images, identifications of nests have been conducted and geographical coordinate locations at nest centers have been calculated. In training and testing, feature pyramid network (FPN) and UNet architectures have been used. Conclusions drawn through deep learning-based image segmentation revealed that the generated nest map can become a beneficial contribution in combating PPM.In Kahramanmaraş, the severity of red pine PPM infestations was evaluated using Landsat 8 OLI satellite imagery and remote sensing techniques. The minimum, average, maximum, and sum NDVI values were calculated for the years before (2016) and after (2022) the PPM infestation. These NDVI values were compared using SPSS statistical software and t-tests, and there was a significant difference between the values calculated before and after the infestation (Özcan and Sivrikaya, 2022).

A review of the literature reveals that the detection of pine processionary moths and similar forest pests has traditionally relied on low-resolution satellite imagery and conventional image processing techniques. For instance, studies by Gooshbor et al. (2016) and Özcan and Sivrikaya (2022) employed NDVI analyses to evaluate forest health at the regional scale. Cardil et al. (2017, 2019) conducted tree-based classifications focused on the severity of damage, reporting accuracy rates between 79% and 81.8%. Ziya et al. (2018) applied classical image processing techniques to detect leaf spot disease but did not incorporate object-based deep learning approaches. More recent studies by Kerkech et al. (2020) and Chen et al. (2021) implemented deep learning-based segmentation methods; however, their research focused respectively on mildew detection in vineyards and optimization of pesticide spraying in agriculture. Akıncı and Göktoğan (2022), on the other hand, focused on mapping PPM nests using Unmanned Aerial Vehicle (UAV) imagery by applying different deep learning architectures.

Taken together, these studies suggest that object-based, high-precision nest detection methods remain relatively underrepresented in the current literature. Addressing this gap, the present study proposes a method that utilizes high-resolution UAV imagery and the YOLOv7 architecture to detect individual nests, with clearly reported accuracy metrics. As part of this study, a custom dataset comprising 700 images collected under real-world conditions was constructed. The model trained using this dataset achieved a mAP@0.5 score of 92.5%. These findings highlight the potential of the proposed approach to contribute to early warning systems, the planning of pest management strategies, and the development of future autonomous monitoring frameworks.

2. Materials and Methods

In this study, the YOLOv7 model was employed for object detection. Since training deep learning models like

YOLOv7 requires substantial computational resources, including high-performance CPUs and GPUs, a cloud-based platform was preferred. Specifically, Google Colaboratory (Google Colab) (Anonymous, 2017) was selected due to its widespread use in artificial intelligence research, its free access to powerful GPU resources, and its compatibility with Python-based deep learning frameworks. The platform's support for the NVIDIA Tesla P100 GPU with 16GB memory provided sufficient computational capacity for training while eliminating the need for dedicated local hardware.

The necessary YOLOv7 configuration files and dependencies were installed within the Colab environment. After annotating the custom dataset, the image and label files were structured in appropriate directories in Google Drive and linked to the Colab runtime. A total of 700 annotated images were prepared, with 560 used for training.

2.1. Creating the Dataset

Utilization of aerial imagery to monitor forest pests is of numerous advantages, offering a more effective and efficient way of doing this compared to the traditional ground-based methods. Getting clear images between trees in rugged terrain can be quite hard to obtain. Additionally, since PPM nests can be found in the upper parts of trees, images were captured using two different UAVs: the DJI Mini 2 and the custom-built UAV (Figure 1). After identifying the area where the nests were found, the drone was flown over the trees, capturing 32 different videos with an integrated RGB camera.

Figure 1. The custom-built UAV employed for image acquisition.

These videos were recorded onto a memory card. Subsequently, a small code written in Python was employed to extract images from the video data, resulting in a total of 500 images. Of these, 400 images (80%) were used for training, while 100 images (20%) were designated for testing. To improve the dataset, the number of frames was extended from 500 to 700 by incorporating additional real images obtained under different lighting conditions and angles. This adjustment maintained the split of 80% for training and 20% for testing. In the final dataset, 560 images were allocated for

training, and 140 images were used for testing. Video recordings obtained from 50 trees containing nests feature a total of 86 different nests. Each frame may contain a single nest or multiple nests. During the recording process, the position of the drone was continually adjusted to capture images from various angles. Additionally, by altering the drone's horizontal and vertical distances from the nests, images were acquired from different elevations and distances. Sample images obtained from the same tree at varying angles and distances are presented in Figure 2.

Figure 2. Sample images of the tree and its nests, captured from various angles and distances, representing the dataset content.

A dataset was created from a stand located approximately 150 meters inside the Isparta-Antalya highway at the 23rd kilometer, roughly 3.5 kilometers from Güneyce village. The coordinates of the area are 37.6503026° latitude and 30.7258255° longitude. The region, which spans 32 hectares and is situated at an elevation of 700 meters above sea level, was scanned. The area selected for data collection was identified as the starting point of the stand due to the higher density of nests present (Figure 3).
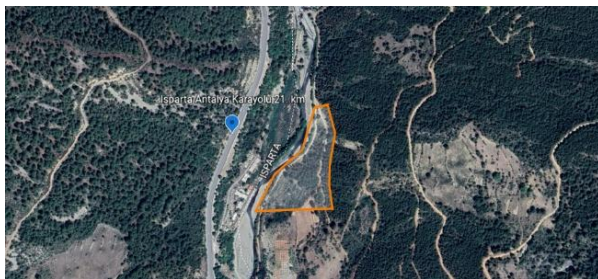

Figure 3. The area from which images were obtained for the dataset.

2.2. YOLO

YOLO, which stands for "You Only Look Once," is a deep learning method. Its first version was developed in 2016 by Joseph Redmon, Ali Farhadi, and Santosh Divvala (Redmon et al., 2016). This architecture enables object classification and detection through the processing of the information in one pass by a convolutional neural network (CNN). YOLO formulates object detection as a regression problem in which one or more bounding boxes and corresponding class probabilities are predicted following a single network pass. Consequently, visual components are processed once to predict the coordinates for every class category (Terven et al., 2023). The YOLO network is more efficient and higher performing than other approaches. By modifying the model size, it can provide a trade-off between performance and accuracy; reducing the model size can increase speed, and enlarging it can produce more precise results (Ali and Zhang, 2024). Figure 4 illustrates the architecture of the original YOLO model, which includes 24 convolutional layers plus 2 fully connected layers (Redmon et al., 2016).
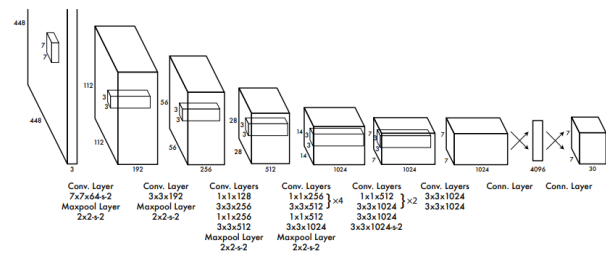

Figure 4. YOLO architecture (Redmon et al., 2016).

Due to its flexible architecture and ability to balance inference speed and detection accuracy, YOLO has become a preferred method in many real-time object detection tasks, especially in resource-constrained environments. In this study, YOLOv7 was selected as the detection backbone, given its high accuracy and improved computational efficiency compared to earlier

YOLO versions and other popular object detectors such as Faster R-CNN, SSD, or EfficientDet (Zhang et al., 2024). While these alternative architectures demonstrate superior detection performance, their increased processing time and hardware requirements limit their applicability to embedded platforms such as the Jetson TX2 or AGX Xavier. Following a detailed comparative analysis of available YOLOv7 variants, the YOLOv7-Tiny model was chosen due to its balanced performance in terms of detection accuracy and real-time suitability for embedded systems. As shown in Table 1, YOLOv7-Tiny is capable of running at 19 FPS on TX2 and 23 FPS on AGX Xavier, making it suitable for real-time deployment in UAV-based scenarios (Işilak et al., 2023).

Table 1. YOLOv7 and YOLOv8 model FPS results (640×640) on TX2, Xavier, and T4 GPUs.

Platform / Model	TX2	AGX Xavier	Tesla T4
V7-Tiny	52.5ms/19FPS	43.0ms/23FPS	11.1ms/90FPS
V7-XL	409.5ms/2FPS	82.3ms/12FPS	28.4ms/35FPS
V8-N		47.8ms/20FPS	10.4ms/96FPS
V8-XL		176ms/6FPS	34.6ms/29FPS

2.3. YOLOv7

YOLOv7, released in July 2022, is the seventh generation of the YOLO family. This neural network has achieved remarkable improvements in detection speed and accuracy compared to its previous ancestors because of some architectural innovations. YOLOv7 methodology attained 56.8% Average Precision (AP) when evaluated on the COCO dataset and exhibited an inference speed of between 5 frames per second (FPS) and 160 FPS and hence a more accurate and faster real-time object detection system compared to its predecessors (Nguyen et al., 2022; Wang et al., 2022).

YOLOv7 is designed using Extended Efficient Layer Aggregation Networks (E-ELAN). E-ELAN, developed based on ELAN architecture, enhances the model's learning capacity by increasing the number of features added through group convolution. Specifically, it ensures efficient parameter utilization through strategies for expanding, shuffling, and merging feature maps (expand, shuffle, merge cardinality). Figure 5 presents the E-ELAN and ELAN architectures (Wang et al., 2022).
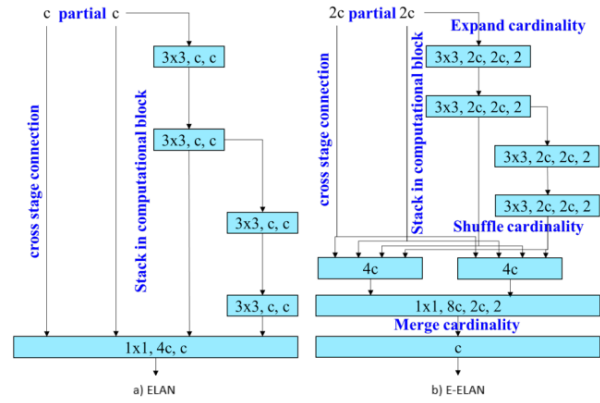

Figure 5. a) ELAN architecture and b) E-ELAN architecture (Wang et al., 2022).

One of the reforms introduced by YOLOv7 is the model scaling method. The primary aim of model scaling is to adjust the core characteristics of the model to meet different application requirements. Through model scaling, the model's width (number of channels), depth (number of stages), and resolution (input image size) can be optimized. Another innovation is the planned reparameterization process. RepConv (Re-parameterized Convolution) is a method that combines multiple kernels within a single convolutional layer with 1x1 and 3x3 convolutions along with an identity connection. Yet, the identity connection part of RepConv has the potential to interfere with the learning mechanisms of other components of architectures such as ResNet and DenseNet. To solve this problem, a variant known as RepConvN was created. RepConvN is a tailored version of RepConv that lacks identity connections, thereby enabling the preservation of parameter efficiency while enhancing model accuracy. Additionally, YOLOv7 has optimized the label assignment process, enhancing prediction consistency across different layers of the model and consequently improving object detection accuracy. The creation of object bounding boxes has also been refined, particularly in accurately detecting overlapping boxes, which is evaluated using the Intersection over Union (IoU) metric (Wang et al., 2022).

For this study, the YOLOv7 framework was implemented. The appropriate hyperparameters for the model were identified, and the training and testing protocols were established. The batch size was set to 16, while the number of epochs was 100. The SiLU (Sigmoid Linear Unit) activation function was integrated with YOLOv7. Data annotation was carried out using the web-based platform "makesense.ai" (Anonymous, 2022).

2.4. Evaluation Metrics

YOLO network employs the Intersection over Union (IoU) metric to calculate how much overlap exists between two bounding boxes. During labeling, bounding boxes are drawn around the targeted object, referred to as the ground truth boxes. As the network begins training, the predicted bounding boxes are generated. The YOLO network compares the ground truth boxes with the

predicted boxes. The greater the overlap between the boxes, the higher the IoU value, which leads to improved detection quality. Conversely, as the IoU value decreases, detection quality declines. The method for calculating IoU is illustrated in Figure 6.
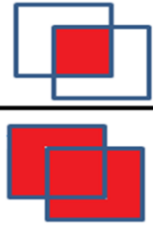

Figure 6. Calculating the IoU Value

For evaluating the training and testing performance of the network, various metrics are available. To calculate these metrics, the values in the confusion matrix must be known. The confusion matrix consists of four values—True Positive (TP), True Negative (TN), False Positive (FP), and False Negative (FN) which quantify the accuracy between actual and predicted classes (Table 2).

Table 2. Confusion Matrix

Confusion Matrix		Actual Values	
		Positive	Negative
Predicted Values	Positive	TP	FP
	Negative	FN	TN

- **TP** refers to instances that are correctly predicted as positive by the model.
- **TN** indicates instances that the model correctly predicts as negative.
- **FP** denotes instances that are incorrectly predicted as positive while being negative.
- **FN** represents instances that are incorrectly predicted as negative while being positive.

Using the values from the confusion matrix, metrics such as Precision, Recall, and F1-score can be calculated (equations 1, 2, 3).

$$Precision = \frac{TP}{TP + FP} \tag{1}$$

$$Recall = \frac{TP}{TP + FN} \tag{2}$$

$$F1_{Score} = 2 \times \frac{Recall \times Prec}{Recall + Prec} \tag{3}$$

One of the most common evaluation metrics in deep learning-based object detection models is the mean Average Precision (mAP) value. The mAP value is computed by averaging the precision and recall performance across all classes. Initially, the Average Precision (AP) for each class is determined using the Precision-Recall curve. The Area Under Curve (AUC) is calculated to obtain the mean precision. Finally, the average of the AP values calculated for all classes yields the mAP value (Equation 4). The "N" in Equation 4 refers to the number of classes. Different mAP metrics exist based on IoU thresholds. For instance, mAP@0.5 indicates the average precision calculated based on results where the IoU value is 0.5 or higher. When expressed as mAP@0.5:.05:.95, it refers to the average of mAP values calculated for IoU values ranging from 0.5 to 0.95, with increments of 0.05 (Padilla et al., 2020).

$$mAP = \frac{1}{N} \sum_{i=1}^{N} AP_i \tag{4}$$

3. Results and Discussion

This study aimed to detect nests containing PPM larvae using a deep learning-based YOLOv7 architecture. The dataset utilized for this purpose is outlined in Section 2.1. Initially, the YOLOv7 network was trained using a dataset consisting of 500 images. Of these images, 400 were allocated for training and 100 for testing. A total of 123 annotations were made in the 100 images designated for testing. The confusion matrix of the model trained with the dataset of 500 images is presented in Figure 7.

The performance metrics, including Precision, Recall, the Precision-Recall curve, and the F1-score graph, of the models trained with 500 and 700 images are presented in Figures 8 and 9, respectively.
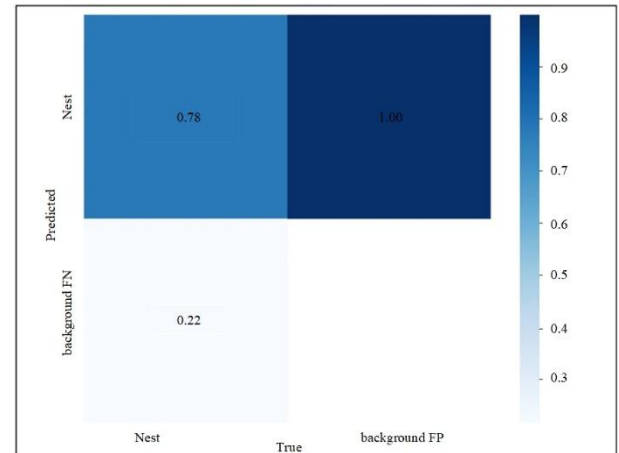

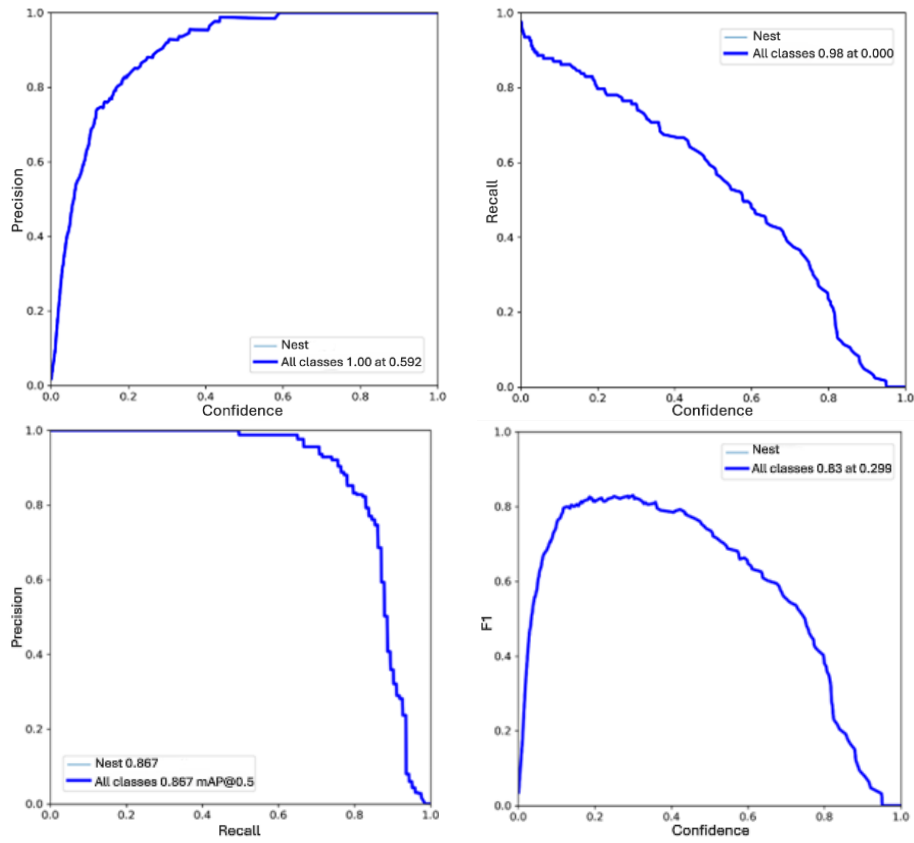**Figure 7.** The confusion matrix of the model trained with 500 images.

Figure 8. The performance metrics of the model trained with 500 images.
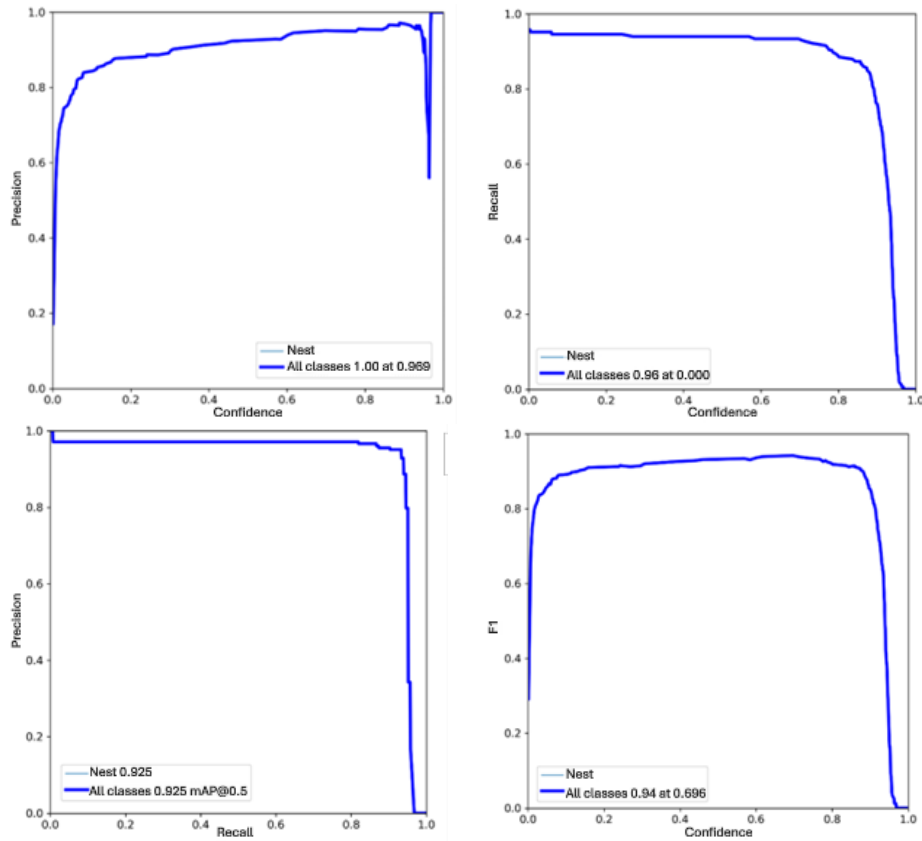

Figure 9. The performance metrics of the model trained with 700 images.

The model trained with a dataset of 500 images exhibited a mean Average Precision at 0.5 (mAP@0.5) value of 0.867. To assess the impact of the number of images in the dataset on success rates, 200 additional images captured at different times of the day were incorporated into the dataset, increasing the total number of images to 700. Of the 700 images captured from the videos, 560 were allocated for training and 140 for testing, following an 80% and 20% split, respectively. The confusion matrix of the model trained with the dataset of 700 images is presented in Figure 10.
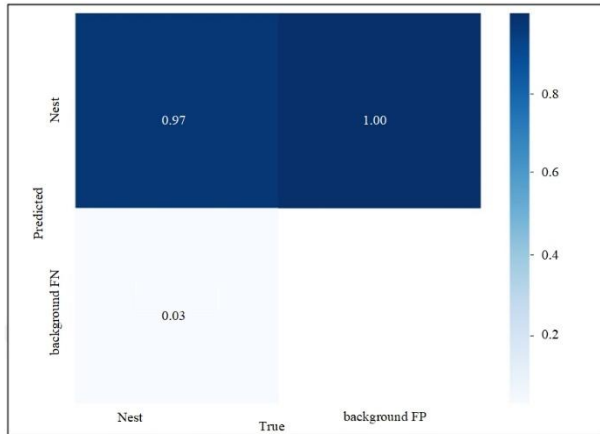

Figure 10. The confusion matrix of the model trained with 700 images.

The training and testing processes conducted with 500 and 700 image datasets revealed that the performance metrics varied despite the constant iteration count. The achieved performance rates are presented in Table 3.

Table 3. Achieved Performance Metrics

Images in Dataset	mAP@0.5	F1-Skor
500	0.867	0.83
700	0.925	0.94

As shown in Table 3, incorporating additional real-world images into the dataset led to a significant improvement in the model's overall performance, particularly in mAP and F1 scores. The inclusion of 200 additional images captured at different times of the day allowed the model to better learn environmental variables such as light angle and intensity. In the initial dataset, intense light reflections occasionally caused the model to misclassify bright surfaces as nests or overlook nests due to low contrast. Including such examples in the training process reduced the model's sensitivity to lighting conditions and improved detection accuracy. However, some limitations remained during field applications. Complex backgrounds, nest-like natural structures, and environmental heterogeneity occasionally led to false positives. Therefore, incorporating background images without any nests into the training process may enable the model to more accurately recognize such patterns, thereby reducing misclassifications particularly related to background elements. These findings suggest that training the model with more diverse and environmentally representative datasets could further enhance detection performance and generalizability. Figure 11 shows sample detections of pine processionary moth nests generated by the model.

From a real-world application perspective, the spatial accuracy of the detected nests is particularly important for operational use, especially in large forested areas. Factors such as flight duration, image resolution, and processing capacity must be taken into account in such contexts. Therefore, it is recommended that the model be integrated with user-friendly interfaces and real-time decision support systems to enhance its practical usability. Furthermore, this study, which focuses on the detection of pine processionary moth nests, could provide greater value to forest management practices if extended to include quantitative analysis of pest density and assessment of damage severity. These enhancements would support the development of more comprehensive and effective intervention strategies in the field.

Figure 11. PPMs detected under different lighting levels and environments.

4. Conclusion

The pine processionary moth is a globally prevalent pest whose population is rapidly increasing due to climate change. In Türkiye, it is commonly found in the Mediterranean, Aegean, Marmara, and Black Sea regions, particularly along the coastal areas. PPM larvae feed on the needles of coniferous trees, causing significant economic and ecological losses in forest ecosystems. Given that a large portion of Türkiye's forests consists of coniferous trees, the risk posed by this pest is considerable. In this regard, a deep learning-based solution was proposed to contribute to the fight against PPM by identifying their nests.

A preliminary custom dataset of 500 images was established to train the YOLOv7 network. The dataset contained nest images captured from different distances and angles and was divided into 80% for training and 20% for testing. The YOLOv7 network was trained and tested using the Google Colaboratory environment. The dataset of 500 images yielded an mAP@0.5 of 0.867 and an F1-score of 0.83. To develop the model further, an additional 200 images captured in different light intensities were included, and the results obtained showed mAP and F1-score improvements. With the increased dataset of 700 images, the mAP@0.5 was 0.925 and the F1-score was 0.94.

The uncontrolled spread of forest pests poses a significant threat to ecosystem health, making their timely and precise detection critically important. This study demonstrates that the developed deep learning-based model can accurately detect PPM nests. Although the current implementation is limited to a single pest species, the model could be extended in future studies to identify multiple pest types by training it on more diverse datasets. Such an enhancement could lay the groundwork for an integrated forest pest monitoring system. In addition, the use of long-term image data may enable the observation of spatial and temporal changes in pest distribution, thus supporting more data-driven intervention planning. Future work should aim to improve the model's generalizability across diverse environmental conditions, reduce false detections through architectural optimizations, and integrate the system with real-time decision support mechanisms. Field testing of the proposed method over larger areas would further contribute to evaluating its operational effectiveness in real-world forestry applications.

Conflict of Interest

The authors declared that there is no conflict of interest.

Ethical Consideration

Ethics committee approval was not required for this study because of there was no study on animals or humans.

References

Akıncı Ş, Göktoğan AH. 2022. An Eco-Friendly Fight Against Thaumetopoea Pityocampa Infestations in Pine Forests Using Deep Learning on UAV Imagery. IEEE, In 2022 Innovations in Intelligent Systems and Applications Conference (ASYU), pp: 1-6.

Ali ML, Zhang Z. 2024. The YOLO framework: A comprehensive review of evolution, applications, and benchmarks in object detection. Computers, 13: 336.

Anonymous. 2016. Orman Bitkisi ve Bitkisel Ürünlerine Arız Olan Zararlı Organizmalar ile Mücadele Yöntemleri. URL: https://www.ogm.gov.tr/tr/e-kutuphane-sitesi/EgitimDokumanlari/Orman%20Zararl%C4%B1lar%C4%B1yla%20M%C3%BCcadele/Orman%20Bitkisi%20ve%20Bitkisel%20%C3%9Cr%C3%BCnlerine%20Ar%C4%B1z%20Olan%20Zararl%C4%B1%20Organizmalar%20ile%20M%C3%BCcadele%20Y%C3%B6ntemleri.pdf. (accessed date: January 14, 2025).

Anonymous. 2017. Google Colab. URL:

https://colab.research.google.com (accessed date: February 09, 2024).

Anonymous. 2022. Get started now. URL: makesense.io (accessed date: January 12, 2025).

Arnaldo PS, Chacim S, Lopes D. 2010. Effects of defoliation by the pine processionary moth Thaumetopoea pityocampa on biomass growth of young stands of Pinus pinaster in northern Portugal. iForest, 3:159.

Avcı M, Altunışık A. 2016. Isparta çam ormanlarında çam kese böceği (Thaumetopoea wilkinsoni Tams, 1926) (Lep.: Notodontidae) zararının artım üzerine etkisi. Türkiye Entomoloji Bülteni, 6:231-244.

Babur H. 2002. Thaumetopoea Pityocampa (Schiff.) Çam Gençliğinde Zarar Miktarı. Ülkemiz Ormanlarında Çam Keseböceği Sorunu ve Çözüm Önerileri Sempozyumu April 24-25, Kahramanmaraş, pp: 37-43.

Çanakçıoğlu H. 1993. Orman Entomolojisi, İstanbul Üniversitesi Orman Fakültesi Yayınları. (pp: 29-36).

Cardil A, Otsu K, Pla M, Silva CA, Brotons L. 2019. Quantifying pine processionary moth defoliation in a pine-oak mixed forest using unmanned aerial systems and multispectral imagery. Plos One, 14: e0213027.

Cardil A, Vepakomma U, Brotons L. 2017. Assessing pine processionary moth defoliation using unmanned aerial systems. Forests, 8:, 402.

Carus S. 2004. Impact of defoliation by the pine processionary moth (Thaumetopoea pityocampa) on radial, height and volume growth of calabrian pine (Pinus brutia) trees in Türkiye. Phytoparasitica, 32: 459-469.

Cebeci HH, Oymen RT, Acer S. 2010. Control of pine processionary moth, Thaumetopoea pityocampa with Bacillus thuringiensis in Antalya, Türkiye. J Environ Biol, 31: 357-361.

Chen CJ, Huang YY, Li YS, Chen YC, Chang CY, Huang YM. 2021. Identification of fruit tree pests with deep learning on embedded drone to achieve accurate pesticide spraying. IEEE Access, 9:21986-21997.

Erkan N. 2011. Impact of pine processionary moth (Thaumetopoea wilkinsoni Tams) on growth of Turkish red pine (Pinus brutia Ten.). Afr J Agric Res, 6: 4983-4988.

Gooshbor L, Bavaghar MP, Amanollahi J, Ghobari H. 2016. Monitoring infestations of oak forests by Tortrix viridana (Lepidoptera: Tortricidae) using remote sensing. Plant Prot Sci, 52: 270-276.

Işilak C, Durmaz O, Şalk Y, Çevılkalp H, Dutağaci H, Gırgın T. 2023. Measuring Electromagnetic Field Strength in Base Stations Using Unmanned Aerial Vehicles. In 2023 31st Signal Processing and Communications Applications Conference (SIU) (pp: 1-4). IEEE.

Kerkech M, Hafiane A, Canals R. 2020. Vine disease detection in UAV multispectral images using optimized image registration and deep learning segmentation approach. Comput Electron Agric, 174:105446.

Nguyen HV, Bae JH, Lee YE, Lee HS, Kwon KR. 2022. Comparison of pre-trained yolo models on steel surface defects detector based on transfer learning with gpu-based embedded devices. Sensors, 22:9926.

Özay FŞ. 2004. Çam keseböceği (Thaumetopoea pityocampa Schiff.) (Lepidoptera-Thaumetopoeidae) ve mücadele yöntemleri. Kavak ve Hızlı Gelişen Orman Ağaçları Araşt. Enst. Müd. Kavakçılık Araştırma Dergisi, 30:55-65.

Özcan GE, Sivrikaya F. 2022. Determining Infestation of Pine Processionary Moth Using Remote Sensing. 4th Intercontinental Geoinformation Days, June 20-21, Tabriz, pp: 99-102.

Özdal MH. 2002. Çam Keseböceği ile Adacıklarla Mücadele Yöntemi, Ülkemiz Ormanlarında Çam Keseböceği Sorunu ve Çözüm Önerileri Sempozyumu Bildiri Kitabı, Kahramanmaraş, pp: 226.

Padilla R, Netto SL, Da Silva EA. 2020. A survey on performance metrics for object-detection algorithms. In *2020 international conference on systems, signals and image processing (IWSSIP)*. IEEE, pp: 237-242.

Redmon J, Divvala S, Girshick R, Farhadi A. 2016. You only look once: Unified, real-time object detection. In Proceedings of the IEEE conference on computer vision and pattern recognition. pp: 779- 788.

Terven J, Córdova-Esparza DM, Romero-González JA. 2023. A comprehensive review of yolo architectures in computer vision: From yolov1 to yolov8 and yolo-nas. Mach Learn Knowl Extr, 5: 1680-1716.

Wang C-Y, Bochkovskiy A, Liao HYM. 2022. YOLOv7: Trainable bag-of-freebies sets new state-of-the-art for real-time object detectors. arXiv. http://arxiv.org/abs/2207.02696.

Yüksel H. 2019. Investigation of the relationship between altitude and biological and ecological characteristics of egg and egg batch in thaumetopoea wilkinsoni tams, 1924 and thaumetopoea pityocampa (den. & schiff., 1775) (lepidoptera: notodontidae) populations. Master's Thesis, Bartın University, Institute of Science, Bartın, pp:59.

Ziya A, Mehmet MO, Yusuf Y. 2018. Determination of Sugar Beet Leaf Spot Disease Level (Cercospora beticola Sacc.) with Image Processing Technique by Using Drone. Curr Inves Agri Curr Res 5 (3)-2018. Mediterranea, 34(3): 149-156.

Zhang Z, Xie X, Guo Q, Xu J. 2024. Improved YOLOv7-Tiny for object detection based on UAV aerial images. Electronics, 13(15): 2969.